



## A: Kinetics, Dynamics, Photochemistry, and Excited States

**Modulating Excited Charge Transfer States of G-Quartet Self-Assemblies by Earth Alkaline Cations and Hydration**

Branislav Milovanovi#, Ivana M. Stankovi#, Milena Petkovic, and Mihajlo Etinski

*J. Phys. Chem. A*, **Just Accepted Manuscript** • DOI: 10.1021/acs.jpca.0c05022 • Publication Date (Web): 16 Sep 2020

Downloaded from pubs.acs.org on September 16, 2020

**Just Accepted**

“Just Accepted” manuscripts have been peer-reviewed and accepted for publication. They are posted online prior to technical editing, formatting for publication and author proofing. The American Chemical Society provides “Just Accepted” as a service to the research community to expedite the dissemination of scientific material as soon as possible after acceptance. “Just Accepted” manuscripts appear in full in PDF format accompanied by an HTML abstract. “Just Accepted” manuscripts have been fully peer reviewed, but should not be considered the official version of record. They are citable by the Digital Object Identifier (DOI®). “Just Accepted” is an optional service offered to authors. Therefore, the “Just Accepted” Web site may not include all articles that will be published in the journal. After a manuscript is technically edited and formatted, it will be removed from the “Just Accepted” Web site and published as an ASAP article. Note that technical editing may introduce minor changes to the manuscript text and/or graphics which could affect content, and all legal disclaimers and ethical guidelines that apply to the journal pertain. ACS cannot be held responsible for errors or consequences arising from the use of information contained in these “Just Accepted” manuscripts.

# Modulating Excited Charge Transfer States of G-Quartet Self-Assemblies by Earth Alkaline Cations and Hydration

Branislav Milovanović,<sup>†</sup> Ivana M. Stanković,<sup>‡</sup> Milena Petković,<sup>†</sup> and Mihajlo Etinski<sup>\*,†</sup>

<sup>†</sup>*Faculty of Physical Chemistry, University of Belgrade*

*Studentski trg 12-16 11000 Belgrade, Serbia*

<sup>‡</sup>*Institute of Chemistry, Technology and Metallurgy, University of Belgrade*

*Njegoševa 12, 11000 Belgrade, Serbia*

E-mail: etinski@ffh.bg.ac.rs, phone: +381113336632

## Abstract

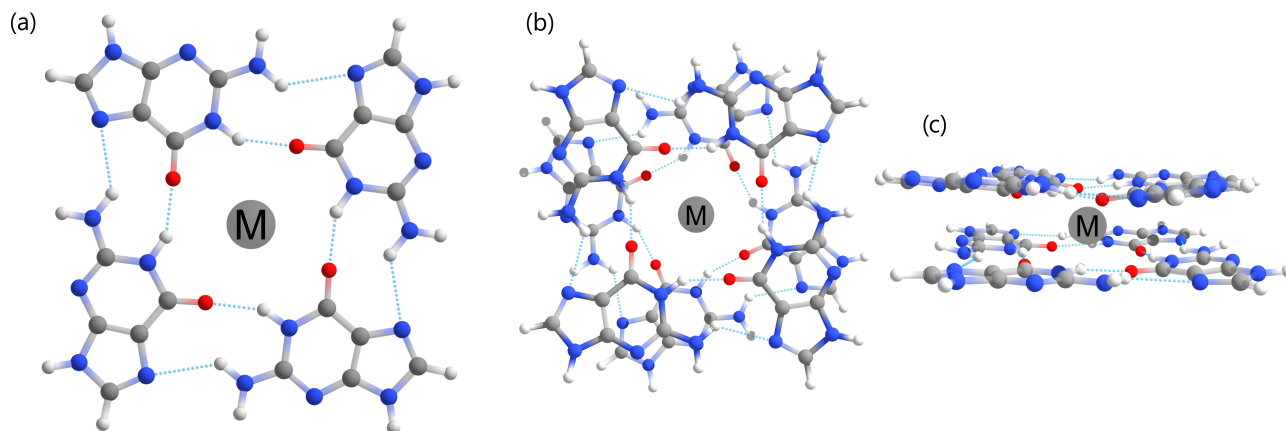
Guanine self-assemblies are promising supramolecular platforms for optoelectronic applications. The study [*J. Phys. Chem. C* **2012** *116* 14682–14689] reported that alkaline cations cannot modulate the electronic absorption spectrum of G-quadruplexes, although a cation effect is observable during electronic relaxation due to different mobility of Na<sup>+</sup> and K<sup>+</sup> cations. In this work, we theoretically examined whether divalent Mg<sup>2+</sup> and Ca<sup>2+</sup> cations and hydration might shift excited charge transfer states of a cation templated stacked G-quartets to the absorption red tail. Our results showed that earth alkaline cations blue-shifted nπ\* states and stabilized charge transfer ππ\* states relative to those of complexes with alkaline cations, although the number of charge separation states was not significantly modified. Earth alkaline cations were

not able to considerably increase the amount of charge transfer states below the  $L_b$  excitonic states. Hydration shifted charge transfer states of  $\text{Na}^+$  coordinated G-octet to the absorption red tail, although this part of the spectrum was still dominated by monomer-like excitations. We found G-octet electron detachment states at low excitation energies in aqueous solution. These states were distributed over a broad range of excitation energies and could be responsible for oxidative damage observed upon UV irradiation of biological G-quadruplexes.

## Introduction

Guanine (G) and its derivatives are able to self-assemble into ribbons and macrocycles formed by four monomers (quartets). In both structures monomers are connected by four hydrogen bonds formed between complementary Watson-Crick and Hoogsteen edges of neighboring units, but their relative stability depends on the experimental conditions.<sup>1</sup> Particularly, monovalent and divalent cations dictate the self-assembly of guanines into a cation templated G-quartet structure (see Figure 1). The stability of this supramolecular structure is determined by cooperative hydrogen bonding, the size of the cation and its hydration energy.<sup>2-9</sup>

Figure (1) (a) Structure of G-quartet coordinated with a metal cation. (b) Top and (c) side view of stacked G-quartet coordinated with a metal cation.



Stacking of G-quartets into columnar aggregates gives rise to G-quadruplexes in which cations are sandwiched between two G-quartets or between every other G-quartet pair as in the case of  $\text{Sr}^{2+}$  cation.<sup>10</sup> The latter binding mode likely occurs due to unfavorable electrostatic repulsion between double positive charges. Among monovalent cations,  $\text{K}^+$  has the strongest ability to govern 5'-guanosine monophosphate self-assembly into G-quadruplexes followed by  $\text{Na}^+$  and  $\text{Rb}^+$ .<sup>11</sup> Generally, divalent cations are known to be more effective in stabilization of G-quadruplexes than alkaline cations.<sup>12,13</sup> Kwan *et al.* found that divalent cation ability to promote formation of a guanosine derivative self-assembly follows the ordering of ionic radii found for monovalent alkaline cations ( $\text{Sr}^{2+} \gg \text{Ba}^{2+} > \text{Ca}^{2+}$ ).<sup>14</sup> G-quadruplexes are also found in guanine rich DNA and RNA sequences and have important biological functions.<sup>15,16</sup> It is possible to form superstructures called G-wires by polymerization of short biological G-quadruplex sequences by gel electrophoresis in the presence of  $\text{K}^+$ ,  $\text{Na}^+$  or  $\text{Mg}^{2+}$  cations.<sup>17</sup>

Self-assembly of functional building blocks into nanometer-sized structures is found to be a more efficient approach for optoelectronic applications than covalent syntheses.<sup>18</sup> Guanine absorbs light in the UV spectral region and it is not suitable for Solar radiation absorption. For photovoltaic applications, it might be functionalized with a dye molecule. Wasielewski and coworkers exploited G-quadruplex decorated with  $\pi$ -chromophores as a supramolecular platform for photochemical charge separation.<sup>19-21</sup> The core-shell columnar architecture of these systems favors photoinduced charge separation over long distance, which demonstrates that G-quadruplexes can serve as effective hole conduits in these assemblies. Pu *et al.* used  $\text{Sr}^{2+}$  templated G-quartet self-assembly of guanosine 5'-monophosphate intercalated with dye molecules as a light-harvesting antenna.<sup>22</sup> This nanostructure showed good light-harvesting properties both in solution and in the solid state indicating the potential for application as a photoelectric device.

Given the growing interest in G-quadruplex-based optoelectronic devices, it is necessary to examine how structural parameters modulate absorption and electronic relaxation

1  
2  
3 of these supramolecular structures. Previous experimental and theoretical studies exam-  
4 ined biological G-quadruplexes and G-wires templated with Na<sup>+</sup> and K<sup>+</sup> cations.<sup>23-38</sup> These  
5 studies found that their photophysics depends on the number of stacked G-quartets, relative  
6 orientation between neighbouring G-quartets and a templating cation. Absorption spectra  
7 of G-quadruplexes are dominated by collective excitations<sup>23</sup> which include Frenkel excitons  
8 and charge transfer states.<sup>32</sup> Excitons are found to be more strongly coupled between stacked  
9 guanines than between hydrogen-bonded guanines.<sup>31,32</sup>

10  
11  
12  
13  
14  
15  
16  
17 Although the G-quadruplex structure is necessary for promoting intramolecular energy  
18 transfer, the templating cations are also needed for the unusually efficient energy transfer  
19 reactions within the G-quadruplex.<sup>25</sup> Hua *et al.* studied absorption and emission spectra of  
20 a short DNA sequence containing G-quadruplexes templated with Na<sup>+</sup> and K<sup>+</sup> cations.<sup>26</sup>  
21 Two-dimensional NMR experiments could not detect any differences in the relative positions  
22 of guanine moieties indicating that the overall structure is not affected by the cation type.  
23 Also, the absorption spectra did not exhibit significant differences in either the shape or  
24 intensity. On the other hand, fluorescence spectra showed remarkable differences since they  
25 were dominated by emission from charge transfer and Frenkel excitons for Na<sup>+</sup> and K<sup>+</sup> tem-  
26 plated structures, respectively. These findings were related to different mobility of Na<sup>+</sup> and  
27 K<sup>+</sup> cations in the central vacancies of G-quadruplexes. More mobile Na<sup>+</sup> cations stabilized  
28 charge transfer states during electronic relaxation, whereas this decay channel is obstructed  
29 by less mobile K<sup>+</sup> cation.

30  
31  
32  
33  
34  
35  
36  
37  
38  
39  
40  
41  
42  
43 In this work, we examined to what extent the absorption spectra of G-quadruplexes  
44 templated with divalent cations differ to those of alkaline cations. Excited charge transfer  
45 states are sensitive to environment polarity and double positive charges of divalent cations  
46 might stabilize them to a greater extent than those of monovalent cations. It is particularly  
47 intriguing whether earth alkaline cations are able to shift charge transfer states below the  
48 first bright state since this might result in a more efficient photoinduced charge separation.  
49 We also studied the hydration effects on the excited state properties of G-quadruplexes.

1  
2  
3 To this end, we simulated electronic absorption spectra of stacked G-quartets (G-octet)  
4 templated with divalent earth alkaline cations  $\text{Mg}^{2+}$  and  $\text{Ca}^{2+}$  in the gas phase. As a  
5 reference, we also examined structures with monovalent alkaline cations  $\text{Li}^+$ ,  $\text{Na}^+$ ,  $\text{K}^+$  as  
6 well as the structure without a cation. These systems represent a minimal model of G-  
7 quartet self-assemblies which is at the same time feasible for computational study. The lack  
8 of a sugar-phosphate backbone enables G-quartets to exhibit various close-energy conformers  
9 and hydrogen bonding patterns.<sup>4</sup> Hence, we computed the ground state nuclear ensemble by  
10 employing classical density functional theory-based molecular dynamics. Subsequently, the  
11 excited states and their properties were calculated using time-dependent density functional  
12 theory. The hydration effects on the excited states were examined by comparing the density  
13 of states of G-octets templated with sodium cation in the gas phase and in the microhydrated  
14 environment.

15  
16  
17 The paper is organized as follows. In the next section, we discuss various computational  
18 methods which were employed in this work. In the following section, we present and discuss  
19 results related to the relative arrangements of guanines in the G-octets as well as the cation  
20 and hydrogen bonding interactions with the carbonyl group. Also, we discuss the density of  
21 excited states, charge transfer character, absorption spectra and hydration effects. Finally,  
22 we draw conclusions from our study.

## 23 24 25 26 27 28 29 30 31 32 33 34 35 36 37 38 39 40 41 42 43 44 45 46 47 48 49 50 51 52 53 54 55 56 57 58 59 60

Density functional theory-based molecular dynamics simulations were performed with the  
CP2K program package.<sup>39</sup> We employed the BLYP functional<sup>40,41</sup> and Grimme's D3 correc-  
tion for dispersion interaction.<sup>42</sup> The electron density was expanded using a mixed Gaussian  
and plane waves method<sup>43</sup> with a DZVP basis set for the localized functions, and a cutoff  
of 320 Ry for the plane waves. GTH pseudopotentials<sup>44</sup> were used to replace core electrons,  
whereas the valence electrons were correlated. The simulation was performed in a cubic box

1  
2  
3 with the edge size of 25 Å under the non-periodic conditions. The SCF convergence was  
4 set to  $5.0 \times 10^{-7}$  in atomic units. The nuclei were propagated on the Born-Oppenheimer  
5 surface of the electronic ground state using a time step of 0.5 fs. The CSVr thermostat<sup>45</sup>  
6 was employed in order to simulate a canonical ensemble at 300 K. The initial geometries for  
7 equilibration were chosen to be anti/anti partial 5/6 ring structure (see Figure 1), which  
8 was reported to be the most common stacking geometry within the G-quadruplex core.<sup>46</sup>  
9 The structures were equilibrated for 2 ps and subsequently propagated for 14 ps in the NVT  
10 ensemble.  
11  
12  
13  
14  
15  
16  
17  
18

19 Electronic absorption spectrum was simulated within the semi-classical approximation in  
20 which it is proportional to an ensemble average of vertical electronic excitations:  
21  
22  
23

$$24 \quad A(\omega) \sim \langle \sum_n f_{n,0} g(\omega - \omega_{n,0}) \rangle, \quad (1)$$

25  
26  
27  
28 where  $f_{n,0}$  and  $\omega_{n,0}$  are the oscillator strength and frequency of the electronic transition to  
29 the  $n$ -th electronic state, respectively, and  $g$  is a line-broadening function with the Gaussian  
30 shape  
31  
32

$$33 \quad g(\omega) = \sqrt{\frac{2}{\pi\delta^2}} \exp(-2\omega^2/\delta^2). \quad (2)$$

34  
35  
36  
37 We used a large broadening value  $\delta = 0.2$  eV, which enables us to remove statistical noise.  
38 The nuclear distribution in the ground electronic state was prepared by molecular dynamics  
39 simulation. The density of transition was determined by taking the equation 1 and substi-  
40 tution  $f_{n,0} = 1$ . Excited electronic states were computed by employing linear response time-  
41 dependent density functional theory with long-range corrected CAM-B3LYP functional<sup>47</sup>  
42 and split valence 6-31G(d) basis set. We calculated 32 excited electronic states at 10 sampled  
43 configuration separated by 1 ps for each G-octet. The excited states calculations were carried  
44 out by using Gaussian software package.<sup>48</sup> Analysis of the excited states was conducted using  
45 TheoDORE program,<sup>49</sup> which evaluates the one-electron transition density matrix<sup>50,51</sup> and  
46 natural transition orbitals (NTOs).<sup>52,53</sup> Excited states of multichromophoric G-octet sys-  
47  
48  
49  
50  
51  
52  
53  
54  
55  
56  
57  
58  
59  
60

1  
2  
3  
4  
5  
6  
7  
8  
9  
10  
11  
12  
13  
14  
15  
16  
17  
18  
19  
20  
21  
22  
23  
24  
25  
26  
27  
28  
29  
30  
31  
32  
33  
34  
tems might be monomer-like excited states, delocalized Frenkel excitons and charge transfer states. Charge transfer states involve transitions between orbitals localized on different guanines. Charge separation states are a subset of charge transfer states in which there is a net charge transfer from one group of guanines to the other. In this work, we only consider charge separation states arising from excitations from one to the other G-quartet. In order to distinguish between locally excited and charge transfer states we used a  $CT$  descriptor implemented in the TheoDORE program, which gives a fraction of the charge transferred between guanines - a value of 1 for the pure charge transfer state and 0 for locally excited state. Point from which the locally excited state turns into the charge transfer state has to be chosen arbitrary and in this work we chose a threshold value of 0.5. Charge separation states were determined by analyzing a  $CT_{net}$  descriptor and two fragments, each consisted of one G-quartet. We also used a threshold value of 0.5 for assigning charge separation character. Delocalization of electronic transitions (the number of guanines which participate in the excitation) was computed by employing  $DEL$  descriptor in the TheoDORE program. This descriptor provided a real value from one up to the number of guanine fragments (eight). The computed values were rounded to the nearest integer.

35  
36  
37  
38  
39  
40  
41  
42  
43  
44  
45  
46  
47  
48  
49  
50  
51  
52  
53  
54  
55  
56  
57  
58  
59  
60  
The configurations of microsolvated cluster used to elucidate the hydration effect were generated by the following procedure. The ten previously selected structures of  $\text{Na}^+$  coordinated G-octet were selected for molecular dynamics simulations in aqueous solution. Each structure was placed in the center of the orthorhombic box and solvated by water molecules using AmberTools20.<sup>54,55</sup> Edges of the box were expanded to a distance of 10 Å away in all directions from the solute, resulting in a box size of around 40, 40 and 31 Å along the x, y and z directions, respectively. The box was filled with 1150 TIP3P<sup>56</sup> water molecules on average. We added one  $\text{Cl}^-$  ion to maintain system electrostatically neutral. The G-octet was described using generalized AMBER force field (GAFF)<sup>57</sup> while  $\text{Na}^+$  and  $\text{Cl}^-$  were described using TIP3P model. The energy of the system was initially minimized by 1000 steps. After minimization, we carried out a 1 ns long classical NVT molecular dynamics run by using



1  
2  
3 NAMD program.<sup>58</sup> The temperature was kept constant at 298 K by means of Langevin dy-  
4 namics method.<sup>59</sup> During the minimization and dynamics, coordinates of G-octet and Na<sup>+</sup>  
5 cation were kept fixed to preserve DFT-MD geometries. This was necessary since GAFF  
6 does not preserve the G-octet structure. The time step for integrating classical equations of  
7 motion was 1 fs. 12 Å cutoff with smooth switching function starting at 10 Å was used  
8 to describe van der Waals forces, whereas electrostatic forces were treated via particle mesh  
9 Ewald method.<sup>60</sup> A microsolvated cluster was created by taking the G-octet structure with  
10 57 closest water molecules from the last configuration of the molecular dynamics run.  
11  
12  
13  
14  
15  
16  
17  
18  
19  
20

## 21 Results and Discussion

### 22 The Ground State Properties

23  
24  
25 The lack of sugar-phosphate backbone in stacked G-quartets gives larger flexibility in rel-  
26 ative arrangements of guanine moieties than those in biological G-quadruplexes. These  
27 arrangements determine dipolar coupling among guanines, which influences the absorption  
28 lineshape. A theoretical study<sup>61</sup> found that the coordination number of Li<sup>+</sup> cation in op-  
29 timized stacked G-quartets differs from other alkaline cations as Li<sup>+</sup> is positioned in the  
30 middle of one G-quartet and it coordinates only four oxygens. This was attributed to small  
31 ionic radius which prevents coordination of all oxygen atoms.<sup>61</sup> In our molecular dynamics  
32 simulations, we observed that Li<sup>+</sup> might interact with both G-quartets. Its most probable  
33 coordination numbers were four and five. We also noticed that Mg<sup>2+</sup> strongly interacted  
34 with six oxygen atoms of which three belong to one G-quartet. Na<sup>+</sup>, K<sup>+</sup> and Ca<sup>+2</sup> cations  
35 were found to be coordinated with eight oxygen atoms, so that oxygen atoms formed square  
36 antiprismatic molecular geometry.  
37  
38  
39  
40  
41  
42  
43  
44  
45  
46  
47  
48  
49  
50

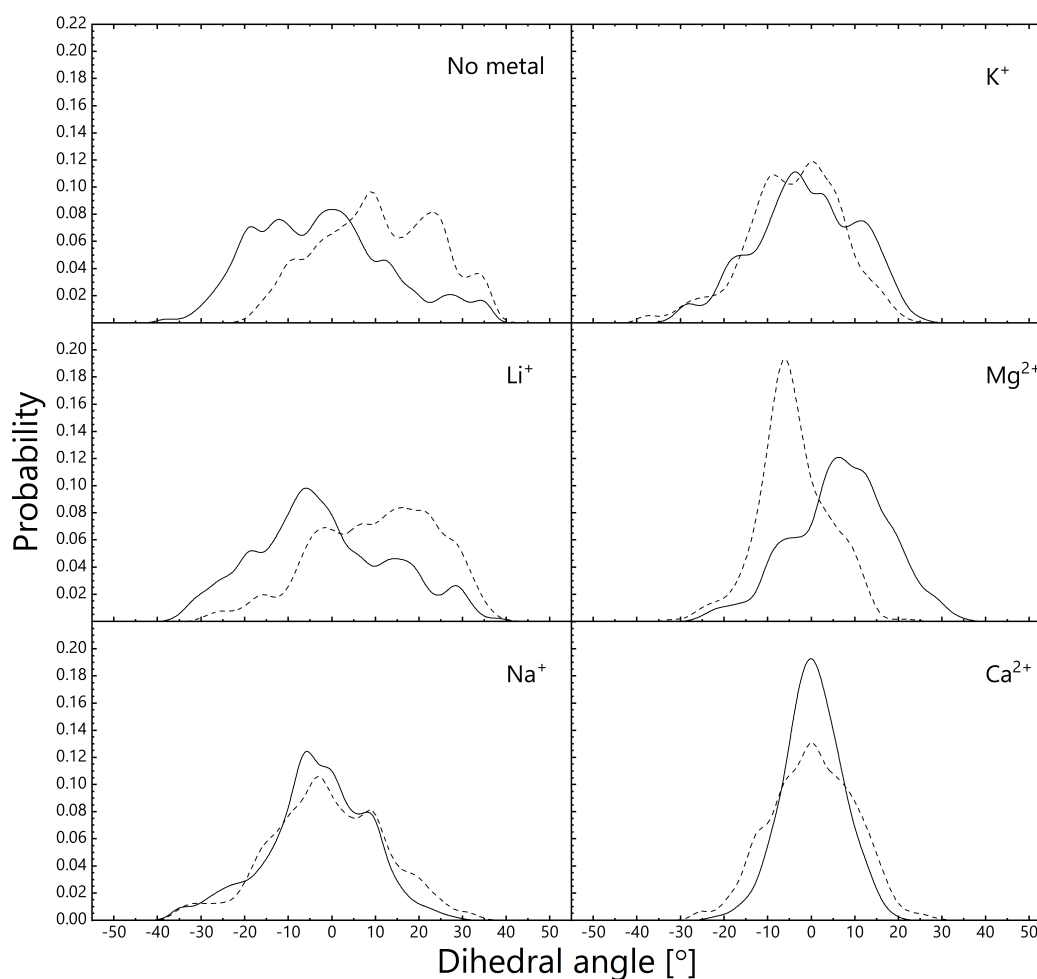
51 Having discussed the coordination of the cations, let us proceed to relative orientation  
52 of guanines in the G-octets. The probability distribution of dihedral angles defined between  
53 the carbonyl oxygen atoms is presented in Figure 2. It reflects a deviation of G-quartet from  
54  
55  
56  
57  
58  
59  
60

1  
2  
3 planarity (dihedral angle equals to zero degrees). The structures with  $\text{Na}^+$ ,  $\text{K}^+$  and  $\text{Ca}^{+2}$   
4 exhibit planar G-quartets,  $\text{Ca}^{+2}$  having the least deviations. The G-octets coordinated with  
5  $\text{Li}^+$ ,  $\text{Mg}^{2+}$  cations and without a cation have G-quartets which are nonplanar. The broad  
6 probability distributions of these systems indicate that they possess shallow potential energy  
7 surface along the dihedral angle. Pronounced asymmetry of the distributions for G-quartets  
8 with  $\text{Li}^+$ ,  $\text{Mg}^{2+}$  cations is due to flexibility of non-coordinated guanines.  
9

10  
11  
12  
13  
14  
15 Azargun et al. failed to produce 9-ethylguanine octet coordinated with  $\text{Li}^+$  cation in  
16 the gas phase, although other alkaline cations easily formed the complexes.<sup>62</sup> We believe  
17 that the instability of  $\text{Li}^+$  coordinated G-octets originates from the inability of  $\text{Li}^+$  cation to  
18 coordinate all oxygen atoms and subsequent the lack of G-quartet rigidity which is crucial  
19 for G-quartet stacking. In the case of  $\text{Mg}^{2+}$  cation, the stability might be even more reduced  
20 since it was previously shown that G-quartets with earth alkaline cations only exist because  
21 of strong cation-guanine attraction<sup>9</sup> and this cation also does not coordinate all oxygen  
22 atoms. We will show below that the earth alkaline cations even reduce the strengths of the  
23 inner hydrogen bonds in the G-octets relative to those of G-octets coordinated with alkaline  
24 cations.  
25  
26  
27  
28  
29  
30  
31  
32  
33  
34

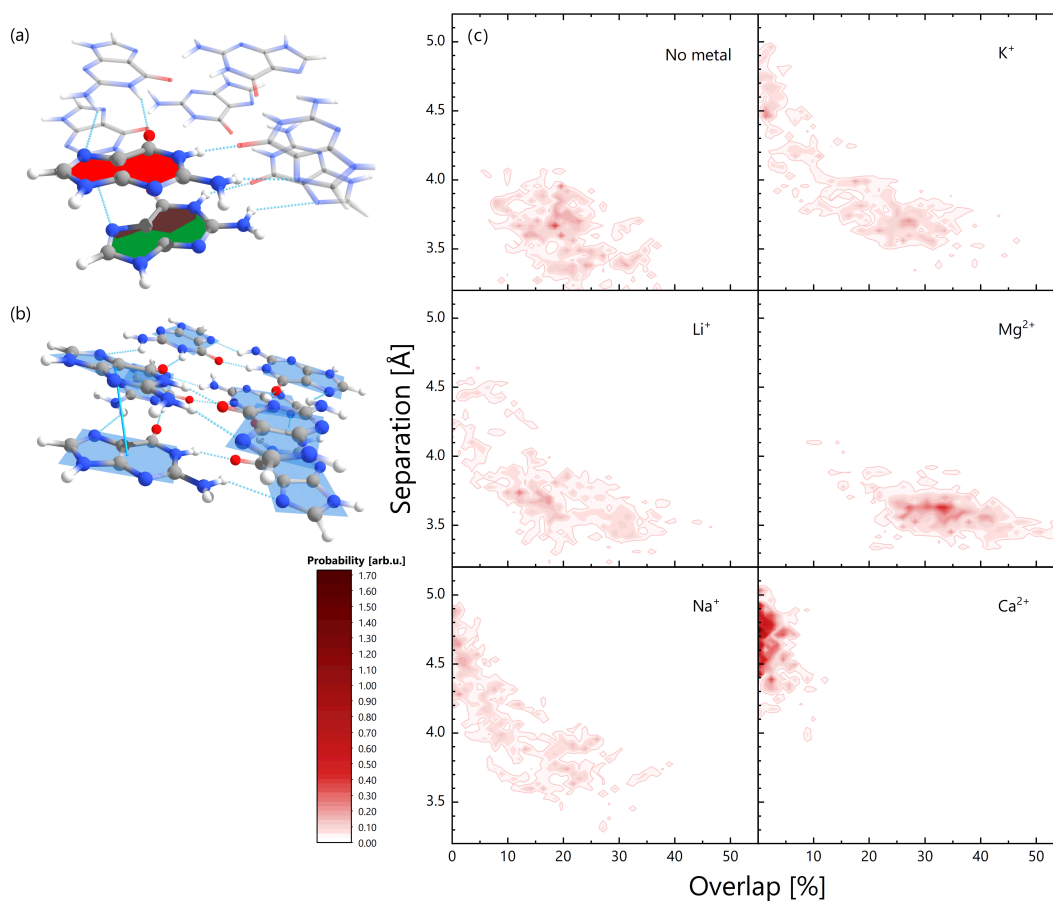
35 G-quartet arrangements which have a high degree of 5/6-ring overlap in G-quadruplexes  
36 exhibit exceptional electron hole transfer rates and charge transfer properties.<sup>29,32</sup> In order  
37 to examine to what extent cations modify guanine stacking in the G-octets, we studied the  
38 following two coordinates: (1) guanine overlap coordinate - defined as an average overlap  
39 between the surfaces enclosed with purine ring atoms obtained by projecting a ring of one  
40 quartet on its counterpart, expressed in percents, (2) guanine separation coordinate - defined  
41 as a minimal distance between geometrical centers of purine rings in one quartet and their  
42 analogues in the other quartet. The probability distribution of these coordinates is given in  
43 Figure 3. It can be noticed that G-octets with alkaline cations have similar distributions,  
44 although the average base separation coordinate is smaller for  $\text{Li}^+$  templating structure than  
45 for the other two structures. In these cases, the guanine overlap coordinates takes values  
46  
47  
48  
49  
50  
51  
52  
53  
54  
55  
56  
57  
58  
59  
60

Figure (2) Probability distributions of the dihedral angles between the carbonyl oxygen atoms for each G-quartet (full and dashed lines).



from 0 to 40 %, with larger values indicating smaller separation. The structure without a metal cation preserves guanine overlap better than the structures with alkaline cations. The highest guanine overlap is found for the  $\text{Mg}^{2+}$  templating G-octet with an average value of 35 %. On the other hand,  $\text{Ca}^{2+}$  cation disrupts base overlap since it does not allow small separations between the bases. These data might indicate that the  $\text{Mg}^{2+}$  containing G-octet would have a higher degree of exciton delocalization in comparison to other G-octets. Yet, we will later show that this is not the case since nonplanar G-quartets in the presence of  $\text{Mg}^{2+}$  cation prevents exciton delocalization.

Figure (3) (a) Schematic display of overlap between the surfaces enclosed with purine ring atoms within a guanine dimer (brown surface). (b) Guanine separation coordinate. (c) Probability distribution of guanine separation and overlap coordinates.



The carbonyl group plays an important role in low-lying electronic excitations of G-octets since these transitions originate from non-bonding  $n$  and bonding  $\pi$  orbitals localized on this group. The electron density of carbonyl is perturbed by inner hydrogen bonds and oxygen-cation interaction. Although the later interaction is dominated by electrostatics<sup>6,9</sup> it also has partially covalent nature. Selected geometrical parameters related to these interactions are collected in the Table 1. Similarly as for the guanine overlap-separation probability distribution, we find that G-octets with alkaline cations have comparable geometrical parameters. The inner hydrogen bonds of alkaline cation coordinated G-octets amount to 1.82 – 1.84 Å, whereas their angles are in the range of 160 – 165 degrees. In the case of

1  
2  
3 earth alkaline cations, the hydrogen bond length is found to be longer. This implies that  
4  
5 G-octets in complexes with earth alkaline cations have weaker inner hydrogen bonds relative  
6  
7 to the alkaline analogues. Particularly, the  $\text{Mg}^{2+}$  coordinated structure has a 0.23 Å longer  
8  
9 inner hydrogen bond than the one in the G-octet without the cation. On the other hand,  
10  
11 earth alkaline cations make the oxygen-cation distance even shorter than the alkaline cations,  
12  
13 which is favorable for electrostatic interaction between lone pairs of the oxygens and cation.  
14  
15 This interaction results in elongation of the oxygen lone pair toward the metal cation and  
16  
17 subsequent stabilization of the oxygen  $n$  orbital. Hence, the excitations from the oxygen  $n$   
18  
19 orbitals will have higher energies in G-octets with earth alkaline than with alkaline cations.  
20

21 Table (1) Selected distances (in Å) and an angle (in degrees):  $\text{O}\cdots\text{M}^{+/2+}$  is the oxygen-  
22  
23 cation distance (in the case without cation, it is the distance between geometrical center of  
24  
25 eight oxygen atoms and oxygen atoms),  $\delta[\text{WC}_{LP}\cdots\text{O}]$  is the distance between a Wannier  
26  
27 center of the oxygen lone pair (directed toward the cation) and oxygen nucleus relative to the  
28  
29 value for the G-octet without a cation,  $\text{N-H}\cdots\text{O}$  is the inner hydrogen bond length,  $\text{N-H-O}$   
30  
31 is the inner hydrogen bond angle.

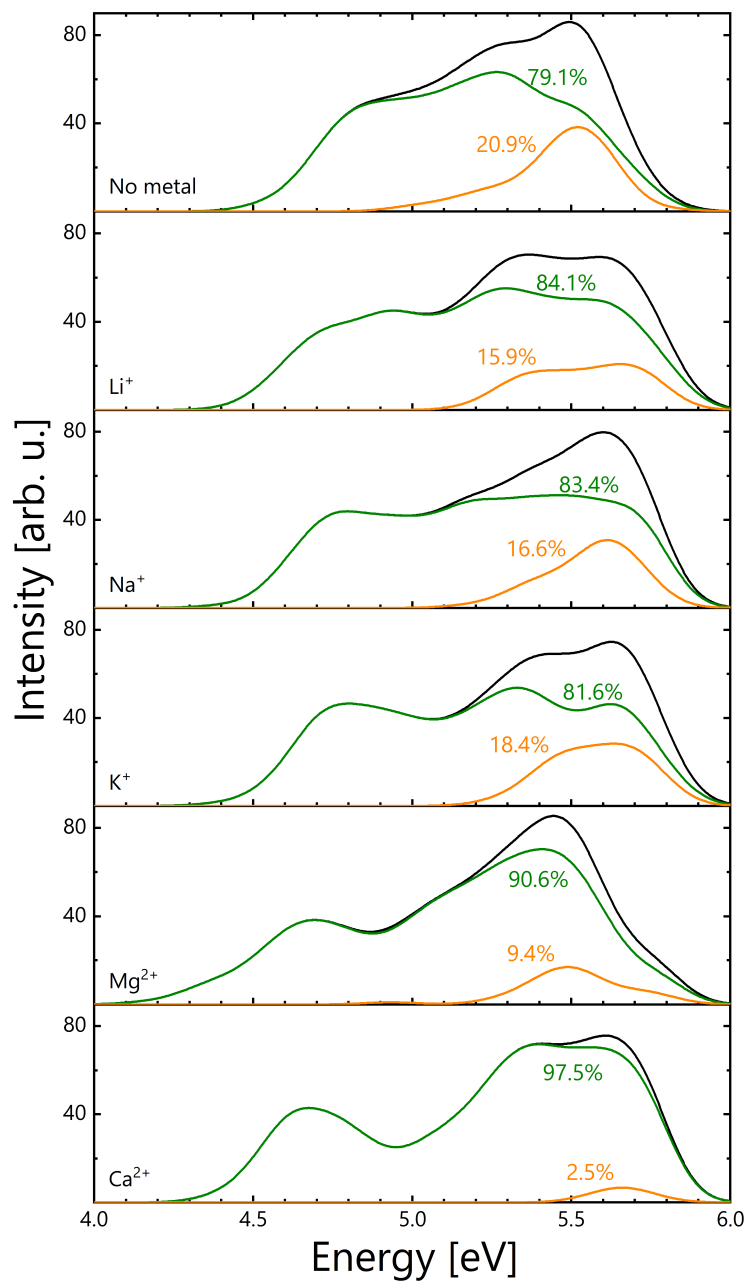
Cation	$\text{O}\cdots\text{M}^{+/2+}$	$\delta[\text{WC}_{LP}\cdots\text{O}]$	$\text{N-H}\cdots\text{O}$	$\text{N-H-O}$
No metal	3.51	0.000	1.96	153
$\text{Li}^+$	2.96	0.011	1.84	160
$\text{Na}^+$	2.77	0.009	1.82	163
$\text{K}^+$	2.93	0.007	1.84	165
$\text{Mg}^{2+}$	2.63	0.028	2.19	146
$\text{Ca}^{2+}$	2.60	0.024	1.88	158

## 32 33 34 35 36 37 38 39 40 41 42 43 44 45 46 47 48 49 50 51 52 53 54 55 56 57 58 59 60

Density of Excited States

Assigning the diabatic character of excited electronic states from each configuration in a nuclear ensemble is a difficult task. A recently proposed procedure for automatic spectral assignment<sup>63</sup> is not applicable due to large discrepancies between the selected reference geometry and other geometries in the ensemble that result from G-octets' pronounced flexibility. Yet, we were able to assign  $n\pi^*$  and  $\pi\pi^*$  transitions by visual inspection of natural transition orbitals.

Figure (4) Density of states (black line) decomposed on the  $\pi\pi^*$  (green line) and  $n\pi^*$  (orange line) contributions.

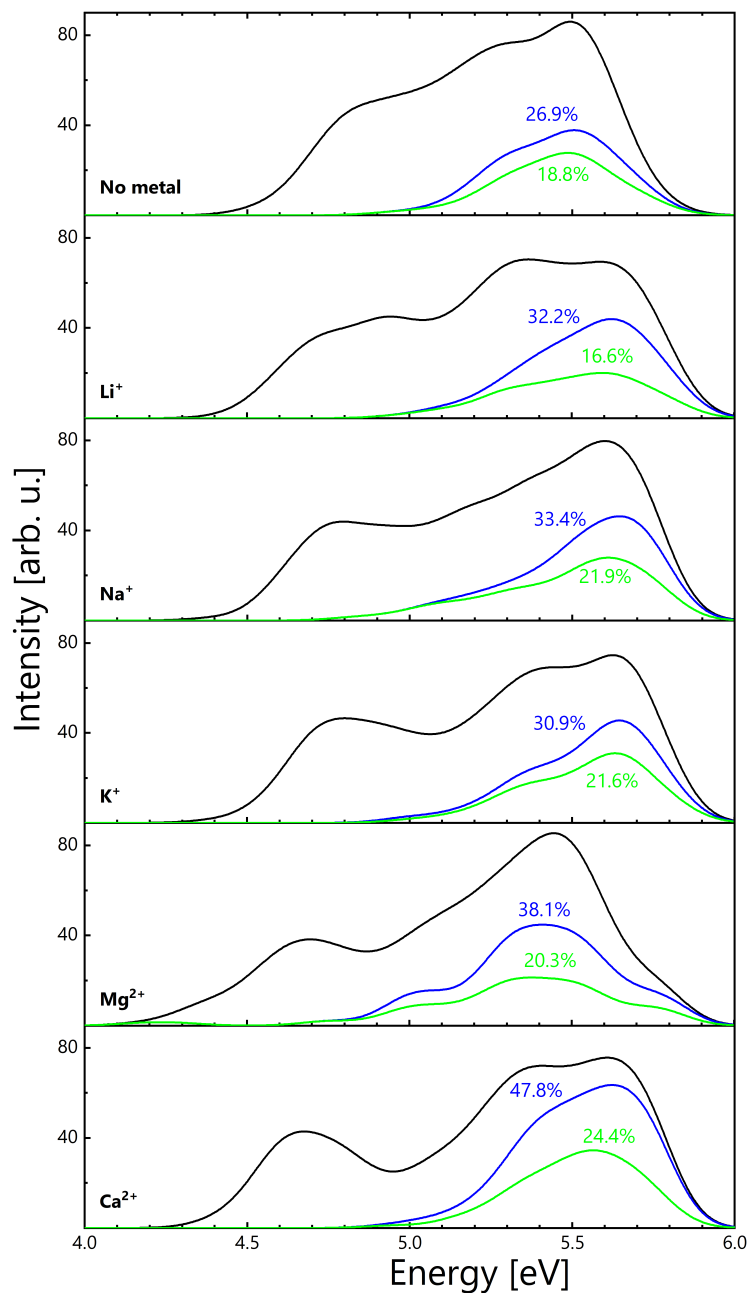


1  
2  
3 The density of states for examined G-octets are given in Figure 4. There is a correlation  
4 between the ground state properties of the G-octets and those densities. As we already  
5 discussed, the ground state properties of the G-octets with alkaline cations are similar. The  
6 same is valid for their densities of states. The situation is somewhat different with earth  
7 alkaline cations. This is in line with a finding of Jissy *et al.* who showed that electronic  
8 properties of a G-quartet are more sensitive to cation radii in the case of earth alkaline  
9 cations than for alkaline cations.<sup>4</sup> Note that the density of states for the Mg<sup>2+</sup> coordinated  
10 G-octet exhibits a long tail at the low-energy side likely due to insufficient sampling in the  
11 nuclear ensemble.  
12  
13  
14  
15  
16  
17  
18  
19  
20

21 In all analyzed systems, most of the first 32 computed excited states belong to  $\pi\pi^*$   
22 excitations. The first two  $\pi\pi^*$  states of guanine are well-known  $L_a$  and  $L_b$  states. By using  
23 the semi-classical approximation, Sapunar *et al.* estimated their energies to be 4.57 and  
24 5.22 eV in the gas phase at ADC(2)/aug-cc-pVDZ level of theory.<sup>63</sup> From the shoulder of  
25 the  $\pi\pi^*$  density of states, we find that  $L_a$  states are positioned at 4.40 eV in the empty  
26 G-octet. The presence of the alkaline and earth alkaline cations red-shifts these states by  
27 0.15 and 0.20 – 0.25 eV, respectively. The energy of the  $L_b$  states amounts to 5.25 eV in  
28 the empty G-octet. The complexation of G-octet with alkaline and earth alkaline cations,  
29 blue-shifts the  $L_b$  states by 0.05 – 0.10 and 0.10 eV, respectively. Interestingly, the  $L_a$  and  $L_b$   
30 states in aqueous solution<sup>63</sup> have the opposite energy shift relative to those due to the cation  
31 complexation in G-quadruplexes. The  $L_a$  and  $L_b$  states are followed with two close-energy  
32 groups of  $\pi\pi^*$  states<sup>63</sup> which are difficult to resolve in our density of states.  
33  
34  
35  
36  
37  
38  
39  
40  
41  
42  
43  
44

45  $n\pi^*$  transitions are found above the  $L_a$  states. Their ratio in the first 32 states decreases  
46 from 21 % in the empty G-octet to 16–18 % in G-octets coordinated with alkaline cations and  
47 9 and 2 % for Mg<sup>2+</sup> and Ca<sup>2+</sup> coordinated complexes, respectively. This is a consequence  
48 of the stabilization of the oxygens'  $n$  orbitals due to hydrogen bonding and interaction  
49 with a cation which results in higher excitation energies of  $n\pi^*$  states. These states are  
50 shifted above the first 32 states and at the same time higher  $\pi\pi^*$  states are lowered to their  
51  
52  
53  
54  
55  
56  
57  
58  
59  
60

Figure (5) Density of states (black line), and its charge transfer (blue line) and charge separation (green line) contributions.





positions. In order to understand the origin of the later effect, we examined charge transfer and charge separation characters of the excited states. Their contributions to the density of states is displayed in Figure 5. Only  $\pi\pi^*$  states above the  $L_a$  states exhibit significant charge transfer character. Their contribution for energies below 5 eV is less than 1 %. The exception is the  $Mg^{2+}$  coordinated G-octet which has approximately 4 % of charge transfer states. The contribution of charge transfer states to density of states of empty G-octet is 27 %. It increases to 31 – 33 % for the G-octets with alkaline cations, which again confirms that Franck-Condon states of these G-octets have very similar properties. An even larger increase is found in the systems coordinated with earth alkaline cations, with 38 and 48 % for  $Mg^{2+}$  and  $Ca^{2+}$ , respectively. Stabilization of these  $\pi\pi^*$  charge transfer states is due to the cation electrostatic field. Contrary to charge transfer states, the total number of charge separation states does not considerably depend on the cation type. The largest number of charge transfer states is observed in the G-octet coordinated with  $Ca^{2+}$  cation - only 2% more than the G-octets with  $Na^+$  and  $K^+$  cations. Thus, it is not possible to employ earth alkaline cations to significantly modulate charge separation in the vertical electronic excitation spectrum. Besides, this finding reveals that additional charge transfer states due to a cation coordination do not have net transfer of charge but are formed from the mutual charge relocations between guanines.

Charge transfer states are typically characterized with low oscillatory strengths. Let us now discuss the absorption spectra and their charge transfer contribution (Figure 6). The absorption spectrum consists of two peaks due to the  $L_a$  and  $L_b$  transitions. These two peaks converge into a single broad peak with a shoulder in the case of the empty G-octet. On the other hand, the gap between them is larger for earth alkaline than for alkaline cations. UV light absorbing charge transfer states are positioned at somewhat higher energies than the maximum of the  $L_b$  band. The contribution of these states to absorption of the empty G-octet is 10 %. Alkaline cations have negligible effects on the charge transfer states absorption, whereas earth alkaline cations increase this contribution by 50 %. These results

1  
2  
3 demonstrate that photoabsorption leads to a more pronounced population of charge transfer  
4 states of earth alkaline complexes compared to their alkaline analogues. Decompositions of  
5 the absorption spectra according to excited state delocalization are given in Figure S1 in  
6 the SI. The absorption is dominated by excited states delocalized on two guanines. The  
7 contribution of states delocalized on three guanines is larger than those of monomer-like  
8 states. The later states contribute at most to the absorption in the red tail, similarly as  
9 in single-stranded polyadenine.<sup>64</sup> We find that that delocalization does not considerably  
10 vary with the cation type. This implies that intramolecular energy transfer occurring upon  
11 photoexcitation of these systems has similar initial dynamics.  
12  
13  
14  
15  
16  
17  
18  
19  
20  
21  
22

## 23 Hydration Effects

24  
25 Charge transfer states in aqueous solution exhibit strong solvatochromism due to dipole  
26 electric field caused by the hydration shell. Yin *et al.* found that the lowest charge transfer  
27 state of stacked adenine in water is red-shifted by 0.7 – 1.0 eV relative to the value in the  
28 gas phase.<sup>65</sup> The charge transfer state is found to be positioned below bright states in the  
29 absorption red tail. Motivated by this finding, we studied hydration effects on charge transfer  
30 states of G-octets templated with Na<sup>+</sup> cation.  
31  
32  
33  
34  
35  
36

37  
38 Figure 7 displays absorption spectra, density of states and their decomposition for the  
39 system in the gas phase and aqueous solution. Both charge transfer and charge separation  
40 states are considerably stabilized in water relative to the gas phase. They appear in the  
41 absorption red tail but their density is lower than monomer-like states. In the blue part of  
42 the spectrum, charge transfer density of states also increases, whereas  $n\pi^*$  states are blue-  
43 shifted. It is interesting that delocalization of excited states in water is larger than in the  
44 gas phase. Particularly, there are two times less monomer-like states and three times more  
45 states that are delocalized on three guanines.  
46  
47  
48  
49  
50  
51  
52

53  
54 Beside charge transfer states localized on the G-octet, we also found charge transfer  
55 states which include electron transfer for the G-octet to water molecules. These electron  
56  
57  
58  
59  
60

1  
2  
3 detachment states have a very broad distribution that begins at 4.4 eV. Their contribution  
4 to the total density of states amounts to 7.5 %, which points to their probable population  
5 upon photoexcitation. In Figure 7, we also provide natural transition orbitals for one such  
6 transition. This is a long-range electron transfer, i. e. an electron is transferred from a  
7 guanine to water molecules that are not in its vicinity.  
8  
9

10  
11  
12  
13 Note that unlike other nucleobases, guanine is very weakly soluble in water. It has  
14 to be functionalized with hydrophilic moieties, such as sugar-phosphate group in order to  
15 become more soluble. Yet, it is not clear to what extent these moieties screen guanines  
16 from water electric field. Nogueira *et al.* showed that charge transfer states of single-  
17 stranded polyadenine in aqueous solution are not located in the red side of the absorption  
18 spectrum.<sup>64</sup> They argued that the sugar-phosphate backbone prevent water molecules to  
19 interact directly with nucleobases and thus small cluster models with hydrated nucleobases  
20 do not appropriately describe hydration of biological self-assemblies.  
21  
22  
23  
24  
25  
26  
27  
28

29 Recently, Markovitsi and coworkers reported that photoionization of biological G-quadruplexes  
30 occurs at much lower energies than for guanine mononucleotide.<sup>37,66</sup> This process is found to  
31 be operative in a very broad excitation energy range. Since the cation effect was noticed,<sup>37</sup>  
32 these authors argued that photoionization of G-quadruplexes does not proceed vertically but  
33 occurs in a series of steps which start from the population of G-quadruplex charge-transfer  
34 states. The similarity between properties of electron detachment states observed in our sim-  
35 ulation and experimentally detected photoionization states of biological G-quadruplexes<sup>37,66</sup>  
36 led us to tentatively propose that G-quadruplex oxidative damage upon UV light absorption  
37 might also take place in a single step.  
38  
39  
40  
41  
42  
43  
44  
45  
46  
47  
48

## 49 Conclusions

50  
51  
52 In this work, the cation and hydration effects on low-energy excited states of G-quartet  
53 self-assemblies in the Franck-Condon region were studied. We employed a minimal model  
54  
55  
56  
57  
58  
59  
60

1  
2  
3 consisting of two stacked G-quartets coordinated with alkaline  $\text{Li}^+$ ,  $\text{Na}^+$ ,  $\text{K}^+$  and earth  
4 alkaline  $\text{Mg}^{2+}$ ,  $\text{Ca}^{2+}$  cations. The lack of a sugar-phosphate backbone in these systems  
5 resulted in larger conformational flexibility of guanine molecules. Generally, all alkaline  
6 cation coordinated G-octets had similar ground state properties. The exception was lower  
7 coordination number of  $\text{Li}^+$  cation, which enabled larger distortions of G-quartets. Also,  
8 the complex with  $\text{Na}^+$  cation had somewhat shorter oxygen-cation distance and stronger  
9 inner hydrogen bonds than the complexes with other alkaline cations. On the other hand,  
10 the G-octets coordinated with earth alkaline cations exhibited larger variations in guanine  
11 arrangements and the inner hydrogen bond strength. Interestingly, it was found that stacked  
12 guanine molecules in the  $\text{Mg}^{2+}$  containing G-octet experience more pronounced overlap than  
13 in any other G-octet.  
14  
15  
16  
17  
18  
19  
20  
21  
22  
23  
24

25 G-octets coordinated with divalent earth alkaline cations had slightly different excited  
26 state properties than their alkaline counterparts. Apart from the larger  $L_a$ - $L_b$  gaps, the  
27 presence of earth alkaline cations blue-shifted  $n\pi^*$  states and stabilized charge transfer  $\pi\pi^*$   
28 states. Yet, the number of states which resulted in charge separation between G-quartets  
29 was not considerably modified upon cation exchange. The ratio of charge transfer states  
30 lower than 5 eV was below 1 % in all G-octets except for the  $\text{Mg}^{2+}$  coordinated one, which  
31 had approximately 4 %. Therefore, earth alkaline cations are not able to increase the density  
32 of charge transfer states in the absorption red tail. The present study unraveled a complex  
33 relation between the properties of the metal cation and the electronic absorption spectra of G-  
34 quadruplexes that might be exploited in the design of novel nanostructures with adjustable  
35 optical properties. In this respect, it would be interesting to study the effects that may  
36 arise from the coordination with trivalent lanthanide metal ions<sup>67</sup> or two divalent cations  
37 coordinated between consecutive G-quartets.  
38  
39  
40  
41  
42  
43  
44  
45  
46  
47  
48  
49  
50

51 Hydration shifted charge transfer states to the absorption red tail. However, this spec-  
52 tral range was dominated by monomer-like excitations as in the gas phase. We found a  
53 broad density of states related to electron transfer from G-octet to water molecules. These  
54  
55  
56  
57  
58  
59  
60

1  
2  
3 electron detachment states might also be present in biological G-quadruplexes, although  
4 sugar-phosphate backbone screens guanines from water electric field. We tentatively pro-  
5 posed that these states are responsible for oxidative damage of G-quadruplexes<sup>37,66</sup> upon  
6 UV photoexcitation.  
7  
8  
9  
10

## 11 12 13 Acknowledgement

14  
15  
16 The research leading to these results has been co-funded by the European Commission under  
17 the H2020 Research Infrastructures contract no. 675121 (project VI-SEEM). B. M., M. P.  
18 and M. E. acknowledge the financial support by Ministry of Education, Science and Techno-  
19 logical Development of Republic of Serbia Contract number: 451-03-68/2020-14/200146 B.  
20 M. acknowledges the Municipality of Arandjelovac (Youth Office) for the financial support.  
21 M. E. thanks Dr. Nađa Došlić (Ruđer Bošković Institute, Zagreb) for useful comments.  
22  
23  
24  
25  
26  
27  
28  
29  
30

## 31 Supporting Information Available

32  
33  
34 Decomposition of absorption spectra according to excited state delocalization. This material  
35 is available free of charge via the Internet at <http://pubs.acs.org/>.  
36  
37  
38  
39

## 40 References

- 41  
42  
43 (1) Davis, J. T.; Spada, G. P. Supramolecular Architectures Generated by Self-Assembly  
44 of Guanosine Derivatives. *Chem. Soc. Rev.* **2007**, *36*, 296–313.  
45  
46  
47  
48 (2) Louit, G.; Hocquet, A.; Ghomi, M.; Meyer, M.; Sühnel, J. Guanine Tetrads Interacting  
49 with Metal Ions. An AIM Topological Analysis of the Electronic Density. *PhysChem-*  
50 *Comm* **2003**, *6*, 1–5.  
51  
52  
53  
54  
55 (3) van Mourik, T.; Dingley, A. J. Characterization of the Monovalent Ion Position and  
56  
57  
58  
59  
60

- Hydrogen-Bond Network in Guanine Quartets by DFT Calculations of NMR Parameters. *Chem. Eur. J.* **2005**, *11*, 6064–6079.
- (4) Jissy, A.; Ashik, U.; Datta, A. Nucleic Acid G-quartets: Insights into Diverse Patterns and Optical Properties. *J. Phys. Chem. C* **2011**, *115*, 12530–12546.
- (5) Fonseca Guerra, C.; Zijlstra, H.; Paragi, G.; Bickelhaupt, F. M. Telomere Structure and Stability: Covalency in Hydrogen Bonds, not Resonance Assistance, Causes Cooperativity in Guanine Quartets. *Chem. Eur. J.* **2011**, *17*, 12612–12622.
- (6) Yurenko, Y. P.; Novotný, J.; Sklenář, V.; Marek, R. Exploring Non-covalent Interactions in Guanine-and Xanthine-based Model DNA Quadruplex Structures: A Comprehensive Quantum Chemical Approach. *Phys. Chem. Chem. Phys.* **2014**, *16*, 2072–2084.
- (7) Paragi, G.; Guerra, C. F. Cooperativity in the Self-Assembly of the Guanine Nucleobase into Quartet and Ribbon Structures on Surfaces. *Chem. Eur. J.* **2017**, *23*, 3042–3050.
- (8) Milovanović, B. Ž.; Petković, M. M.; Etinski, M. R. Properties of the Excited Electronic States of Guanine Quartet Complexes with Alkali Metal Cations. *J. Serb. Chem. Soc.* **2020**, *85*, 1021–1032.
- (9) Milovanović, B.; Stanojević, A.; Etinski, M.; Petković, M. Intriguing Intermolecular Interplay in Guanine Quartet Complexes with Alkali and Alkaline Earth Cations. *J. Phys. Chem. B* **2020**, *124*, 3002–3014.
- (10) J. Deng, Y. X.; Sundaralingam, M. X-Ray Analysis of an RNA Tetraplex (UGGGGU)<sub>4</sub> with Divalent Sr<sup>2+</sup> Ions at Subatomic Resolution (0.61 Å). *Proc. Natl. Acad. Sci. U.S.A.* **2001**, *98*, 13665–13670.
- (11) Pinnavaia, T. J.; Marshall, C. L.; Mettler, C. M.; Fisk, C. L.; Miles, H. T.; Becker, E. D. Alkali Metal Ion Specificity in the Solution Ordering of a Nucleotide, 5'-Guanosine Monophosphate. *J. Am. Chem. Soc.* **1978**, *100*, 3625–3627.

- 1  
2  
3 (12) Chen, F. M. Sr<sup>2+</sup> Facilitates Intermolecular G-Quadruplex Formation of Telomeric  
4 Sequences. *Biochemistry* **1992**, *31*, 3769–3776.  
5  
6  
7  
8 (13) Hardin, C. C.; Watson, T.; Corregan, M.; Bailey, C. Cation-Dependent Transition  
9 Between the Quadruplex and Watson-Crick Hairpin Forms of d(CGCG3GCG). *Bio-*  
10 *chemistry* **1992**, *31*, 833–841.  
11  
12  
13  
14 (14) Kwan, I. C.; She, Y.-M.; Wu, G. Nuclear Magnetic Resonance and Mass Spectrometry  
15 Studies of 2',3',5'-O-Triacetylguanosine Self-Assembly in the Presence of Alkaline Earth  
16 Metal Ions (Ca<sup>2+</sup>, Sr<sup>2+</sup>, Ba<sup>2+</sup>). *Can. J. Chem.* **2011**, *89*, 835–844.  
17  
18  
19  
20  
21 (15) Blackburn, E. H. Telomeres: No End in Sight. *Cell* **1994**, *77*, 621–623.  
22  
23  
24 (16) Wright, W. E.; Tesmer, V. M.; Huffman, K. E.; Levene, S. D.; Shay, J. W. Normal  
25 Human Chromosomes Have Long G-rich Telomeric Overhangs At One End. *Genes*  
26 *Dev.* **1997**, *11*, 2801–2809.  
27  
28  
29  
30  
31 (17) Davis, J. T. G-Quartets 40 Years Later: From 5'-GMP to Molecular Biology and  
32 Supramolecular Chemistry. *Angew. Chem. Int. Ed.* **2004**, *43*, 668–698.  
33  
34  
35  
36 (18) Wasielewski, M. R. Self-Assembly Strategies for Integrating Light Harvesting and  
37 Charge Separation in Artificial Photosynthetic Systems. *Acc. Chem. Res.* **2009**, *42*,  
38 1910–1921.  
39  
40  
41  
42 (19) Wu, Y.-L.; Brown, K. E.; Wasielewski, M. R. Extending Photoinduced Charge  
43 Separation Lifetimes by Using Supramolecular Design: Guanine-Perylendiimide G-  
44 Quadruplex. *J. Am. Chem. Soc.* **2013**, *135*, 13322–13325.  
45  
46  
47  
48  
49 (20) Wu, Y.-L.; Brown, K. E.; Gardner, D. M.; Dyar, S. M.; Wasielewski, M. R. Photoin-  
50 duced Hole Injection into a Self-Assembled  $\pi$ -Extended G-Quadruplex. *J. Am. Chem.*  
51 *Soc.* **2015**, *137*, 3981–3990.  
52  
53  
54  
55  
56  
57  
58  
59  
60

- 1  
2  
3  
4 (21) Powers-Riggs, N. E.; Zuo, X.; Young, R. M.; Wasielewski, M. R. Symmetry-Breaking  
5 Charge Separation in a Nanoscale Terrylenediimide Guanine-Quadruplex Assembly. *J.*  
6 *Am. Chem. Soc.* **2019**, *141*, 17512–17516.  
7  
8  
9  
10 (22) Pu, F.; Wu, L.; Ran, X.; Ren, J.; Qu, X. G-Quartet-Based Nanostructure for Mimicking  
11 Light-Harvesting Antenna. *Angew. Chem. Int. Ed.* **2015**, *54*, 892–896.  
12  
13  
14 (23) Miannay, F.-A.; Banyasz, A.; Gustavsson, T.; Markovitsi, D. Excited States and Energy  
15 Transfer in G-Quadruplexes. *J. Phys. Chem. C* **2009**, *113*, 11760–11765.  
16  
17  
18  
19 (24) Changenet-Barret, P.; Emanuele, E.; Gustavsson, T.; Improta, R.; Kotlyar, A. B.;  
20 Markovitsi, D.; Vaya, I.; Zakrzewska, K.; Zikich, D. Optical Properties of Guanine  
21 Nanowires: Experimental and Theoretical Study. *J. Phys. Chem. C* **2010**, *114*, 14339–  
22 14346.  
23  
24  
25  
26  
27  
28 (25) Dumas, A.; Luedtke, N. W. Cation-Mediated Energy Transfer in G-Quadruplexes Re-  
29 vealed by an Internal Fluorescent Probe. *J. Am. Chem. Soc.* **2010**, *132*, 18004–18007.  
30  
31  
32  
33 (26) Hua, Y.; Changenet-Barret, P.; Improta, R.; Vayá, I.; Gustavsson, T.; Kotlyar, A. B.;  
34 Zikich, D.; Šket, P.; Plavec, J.; Markovitsi, D. Cation Effect on the Electronic Ex-  
35 cited States of Guanine Nanostructures Studied by Time-Resolved Fluorescence Spec-  
36 troscopy. *J. Phys. Chem. C* **2012**, *116*, 14682–14689.  
37  
38  
39  
40  
41  
42 (27) Rosu, F.; Gabelica, V.; De Pauw, E.; Antoine, R.; Broyer, M.; Dugourd, P. UV Spec-  
43 troscopy of DNA Duplex and Quadruplex Structures in the Gas Phase. *J. Phys. Chem.*  
44 *A* **2012**, *116*, 5383–5391.  
45  
46  
47  
48  
49 (28) Hua, Y.; Changenet-Barret, P.; Gustavsson, T.; Markovitsi, D. The Effect of Size on the  
50 Optical Properties of Guanine Nanostructures: A Femtosecond to Nanosecond Study.  
51 *Phys. Chem. Chem. Phys.* **2013**, *15*, 7396–7402.  
52  
53  
54  
55  
56  
57  
58  
59  
60



- 1  
2  
3 (29) Lech, C. J.; Phan, A. T.; Michel-Beyerle, M.-E.; Voityuk, A. A. Electron-Hole Transfer  
4 in G-Quadruplexes with Different Tetrad Stacking Geometries: A Combined QM and  
5 MD Study. *J. Phys. Chem. B* **2013**, *117*, 9851–9856.  
6  
7  
8  
9  
10 (30) Changenet-Barret, P.; Hua, Y.; Markovitsi, D. Electronic Excitations in Guanine  
11 Quadruplexes. *Top Curr Chem.* **2014**, *356*, 183–201.  
12  
13  
14 (31) Improta, R. Quantum Mechanical Calculations Unveil the Structure and Properties of  
15 the Absorbing and Emitting Excited Electronic States of Guanine Quadruplex. *Chem.*  
16 *Eur. J.* **2014**, *20*, 8106–8115.  
17  
18  
19  
20 (32) Lech, C. J.; Phan, A. T.; Michel-Beyerle, M.-E.; Voityuk, A. A. Influence of Base Stack-  
21 ing Geometry on the Nature of Excited States in G-quadruplexes: A Time-Dependent  
22 DFT Study. *J. Phys. Chem. B* **2015**, *119*, 3697–3705.  
23  
24  
25  
26  
27 (33) Banyasz, A.; Martínez-Fernández, L.; Balty, C.; Perron, M.; Douki, T.; Improta, R.;  
28 Markovitsi, D. Absorption of Low-Energy UV Radiation by Human Telomere G-  
29 Quadruplexes Generates Long-Lived Guanine Radical Cations. *J. Am. Chem. Soc.*  
30 **2017**, *139*, 10561–10568.  
31  
32  
33  
34  
35 (34) Martínez-Fernández, L.; Banyasz, A.; Markovitsi, D.; Improta, R. Topology Controls  
36 the Electronic Absorption and Delocalization of Electron Holes in Guanine Quadru-  
37 plexes. *Chem. Eur. J.* **2018**, *24*, 15185–15189.  
38  
39  
40  
41  
42 (35) Martínez-Fernández, L.; Changenet, P.; Banyasz, A.; Gustavsson, T.; Markovitsi, D.;  
43 Improta, R. Comprehensive Study of Guanine Excited State Relaxation and Photore-  
44 activity in G-quadruplexes. *J. Phys. Chem. Lett.* **2019**, *10*, 6873–6877.  
45  
46  
47  
48  
49 (36) Banyasz, A.; Balanikas, E.; Martinez-Fernandez, L.; Baldacchino, G.; Douki, T.; Im-  
50 prota, R.; Markovitsi, D. Radicals Generated in Tetramolecular Guanine Quadruplexes  
51 by Photoionization: Spectral and Dynamical Features. *J. Phys. Chem. B* **2019**, *123*,  
52 4950–4957.  
53  
54  
55  
56  
57  
58  
59  
60

- 1  
2  
3  
4 (37) Behmand, B.; Balanikas, E.; Martinez-Fernandez, L.; Improta, R.; Banyasz, A.; Bal-  
5 dacchino, G.; Markovitsi, D. Potassium Ions Enhance Guanine Radical Generation upon  
6 Absorption of Low-Energy Photons by G-Quadruplexes and Modify Their Reactivity.  
7 *J. Phys. Chem. Lett.* **2020**, *11*, 1305–1309.  
8  
9  
10  
11  
12 (38) Martínez-Fernández, L.; Esposito, L.; Improta, R. Studying the Excited Electronic  
13 States of Guanine Rich DNA Quadruplexes by Quantum Mechanical Methods: Main  
14 Achievements and Perspectives. *Photochem. Photobiol. Sci.* **2020**, *19*, 436–444.  
15  
16  
17  
18 (39) VandeVondele, J.; Krack, M.; Mohamed, F.; Parrinello, M.; Chassaing, T.; Hutter, J.  
19 QUICKSTEP: Fast and Accurate Density Functional Calculations using a Mixed Gaus-  
20 sian and Plane Waves Approach. *J. Comp. Phys. Comm.* **2005**, *167*, 103–128.  
21  
22  
23  
24 (40) Becke, A. D. Density-Functional Exchange-Energy Approximation with Correct  
25 Asymptotic-Behavior. *Phys. Rev. A* **1988**, *38*, 3098–3100.  
26  
27  
28  
29 (41) Lee, C. T.; Yang, W. T.; Parr, R. G. Development of the Coll-Salvetti Correlation-  
30 Energy Formula into a Functional of the Electron-density. *Phys. Rev. B* **1988**, *37*,  
31 785–789.  
32  
33  
34  
35 (42) Grimme, S.; Antony, J.; Ehrlich, S.; Krieg, H. A Consistent and Accurate Ab Ini-  
36 tio Parametrization of Density Functional Dispersion Correction (DFT-D) for the 94  
37 Elements H-Pu. *J. Chem. Phys.* **2010**, *132*, 154104.  
38  
39  
40  
41 (43) Lippert, G.; Hutter, J.; Parrinello, M. A Hybrid Gaussian and Plane Wave Density  
42 Functional Scheme. *Mol. Phys.* **1997**, *92*, 477–487.  
43  
44  
45  
46 (44) Goedecker, S.; Teter, M.; Hutter, J. Separable Dual-Space Gaussian Pseudopotentials.  
47 *Phys. Rev. B* **1996**, *54*, 1703–1710.  
48  
49  
50  
51 (45) Bussi, G.; Donadio, D.; Parrinello, M. Canonical Sampling Through Velocity Rescaling.  
52 *J. Chem. Phys.* **2007**, *126*, 014101.  
53  
54  
55  
56  
57  
58  
59  
60

- 1  
2  
3 (46) Lech, C. J.; Heddi, B.; Phan, A. T. Guanine Base Stacking in G-quadruplex Nucleic  
4 Acids. *Nucleic Acids Res.* **2012**, *41*, 2034–2046.  
5  
6  
7  
8 (47) Yanai, T.; Tew, D. P.; Handy, N. C. A New Hybrid Exchange-Correlation Functional  
9 Using the Coulomb-Attenuating Method (CAM-B3LYP). *Chem. Phys. Lett* **2004**, *393*,  
10 51–57.  
11  
12  
13  
14 (48) Frisch, M. J.; Trucks, G. W.; Schlegel, H. B.; Scuseria, G. E.; Robb, M. A.; Cheese-  
15 man, J. R.; Scalmani, G.; Barone, V.; Mennucci, B.; Petersson, G. A.; et al., Gaussian 09  
16 Revision D.01. Gaussian Inc. Wallingford CT 2009.  
17  
18  
19  
20 (49) Plasser, F. TheoDORE: a Toolbox for a Detailed and Automated Analysis of Electronic  
21 Excited State Computations. *J. Chem. Phys.* **2020**, *152*, 084108.  
22  
23  
24  
25 (50) Plasser, F.; Lischka, H. Analysis of Excitonic and Charge Transfer Interactions from  
26 Quantum Chemical Calculations. *J. Chem. Theory Comput.* **2012**, *8*, 2777–2789.  
27  
28  
29  
30 (51) Plasser, F.; Wormit, M.; Dreuw, A. New Tools for the Systematic Analysis and Visu-  
31 alization of Electronic Excitations. I. Formalism. *J. Chem. Phys.* **2014**, *141*, 024106.  
32  
33  
34  
35 (52) Mai, S.; Plasser, F.; Dorn, J.; Fumanal, M.; Daniel, C.; González, L. Quantitative Wave  
36 Function Analysis for Excited States of Transition Metal Complexes. *Coord. Chem. Rev.*  
37 **2018**, *361*, 74–97.  
38  
39  
40  
41 (53) Plasser, F. Entanglement Entropy of Electronic Excitations. *J. Chem. Phys.* **2016**, *144*,  
42 194107.  
43  
44  
45  
46 (54) Case, D.; Belfon, K.; Ben-Shalom, I.; Brozell, S.; Cerutti, D.; Cheatham, T.;  
47 Cruzeiro, V.; Darden, T.; Duke, R.; Giambasu, G.; et al., AMBER 2020. University of  
48 California, San Francisco.  
49  
50  
51  
52 (55) Salomon-Ferrer, R.; Case, D. A.; Walker, R. C. An Overview of the Amber Biomolecular  
53 Simulation Package. *WIREs Comput. Mol. Sci.* **2013**, *3*, 198–210.  
54  
55  
56  
57  
58  
59  
60

- 1  
2  
3 (56) Jorgensen, W. L.; Chandrasekhar, J.; Madura, J. D.; Impey, R. W.; Klein, M. L.  
4 Comparison of Simple Potential Functions for Simulating Liquid Water. *J. Chem. Phys.*  
5 **1983**, *79*, 926–935.  
6  
7  
8  
9  
10 (57) Wang, J.; Wolf, R. M.; Caldwell, J. W.; Kollman, P. A.; Case, D. A. Development and  
11 Testing of a General Amber Force Field. *J. Comp. Chem.* **2004**, *25*, 1157–1174.  
12  
13  
14 (58) Phillips, J. C.; Braun, R.; Wang, W.; Gumbart, J.; Tajkhorshid, E.; Villa, E.;  
15 Chipot, C.; Skeel, R. D.; Kalé, L.; Schulten, K. Scalable Molecular Dynamics with  
16 NAMD. *J. Comp. Chem.* **2005**, *26*, 1781–1802.  
17  
18  
19 (59) Martyna, G. J. Remarks on "Constant-Temperature Molecular Dynamics with Momen-  
20 tum Conservation". *Phys. Rev. E* **1994**, *50*, 3234.  
21  
22  
23 (60) Darden, T.; York, D.; Pedersen, L. Particle Mesh Ewald: An N-log(N) Method for  
24 Ewald Sums in Large Systems. *J. Chem. Phys.* **1993**, *98*, 10089–10092.  
25  
26  
27 (61) Zaccaria, F.; Paragi, G.; Fonseca Guerra, C. The Role of Alkali Metal Cations in the  
28 Stabilization of Guanine Quadruplexes: Why K<sup>+</sup> is the Best. *Phys. Chem. Chem. Phys.*  
29 **2016**, *18*, 20895–20904.  
30  
31  
32 (62) Azargun, M.; Jami-Alahmadi, Y.; Fridgen, T. The Intrinsic Stabilities and Structures  
33 of Alkali Metal Cationized Guanine Quadruplexes. *Phys. Chem. Chem. Phys.* **2017**,  
34 *19*, 1281–1287.  
35  
36  
37 (63) Sapunar, M.; Domcke, W.; Došlić, N. UV Absorption Spectra of DNA Bases in the  
38 350-190 nm Range: Assignment and State Specific Analysis of Solvation Effects. *Phys.*  
39 *Chem. Chem. Phys.* **2019**, *21*, 22782–22793.  
40  
41  
42 (64) Nogueira, J. J.; Plasser, F.; González, L. Electronic Delocalization, Charge Transfer  
43 and Hypochromism in the UV Absorption Spectrum of Polyadenine Unravalled by  
44  
45  
46  
47  
48  
49  
50  
51  
52  
53  
54  
55  
56  
57  
58  
59  
60

- 1  
2  
3 Multiscale Computations and Quantitative Wavefunction Analysis. *Chem. Sci.* **2017**,  
4 8, 5682–5691.  
5  
6  
7  
8 (65) Yin, H.; Ma, Y.; Mu, J.; Liu, C.; Rohlfing, M. Charge-Transfer Excited States in  
9 Aqueous DNA: Insights from Many-Body Green's Function Theory. *Phys. Rev. Lett.*  
10 **2014**, *112*, 228301.  
11  
12  
13  
14 (66) Balanikas, E.; Banyasz, A.; Douki, T.; Baldacchino, G.; Markovitsi, D. Guanine Rad-  
15 icals Induced in DNA by Low-Energy Photoionization. *Acc. Chem. Res.* **2020**, *53*,  
16 1511–1519.  
17  
18  
19  
20  
21 (67) Kwan, I. C. M.; She, Y.-M.; Wu, G. Trivalent Lanthanide Metal Ions Promote Forma-  
22 tion of Stacking G-Quartets. *Chem. Commun.* **2007**, 4286–4288.  
23  
24  
25  
26  
27  
28  
29  
30  
31  
32  
33  
34  
35  
36  
37  
38  
39  
40  
41  
42  
43  
44  
45  
46  
47  
48  
49  
50  
51  
52  
53  
54  
55  
56  
57  
58  
59  
60

## Graphical TOC Entry

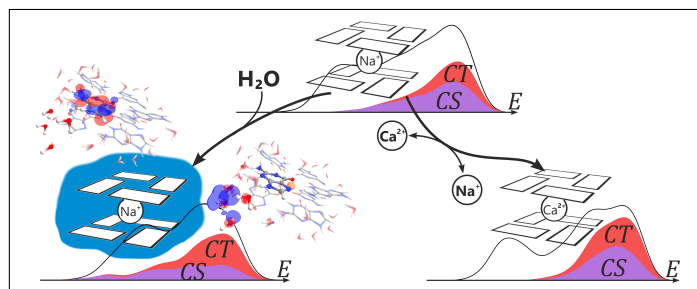


Figure (6) Computed absorption convoluted and stick spectra (black lines), their CT contributions (red lines) and density of states (gray shaded area).

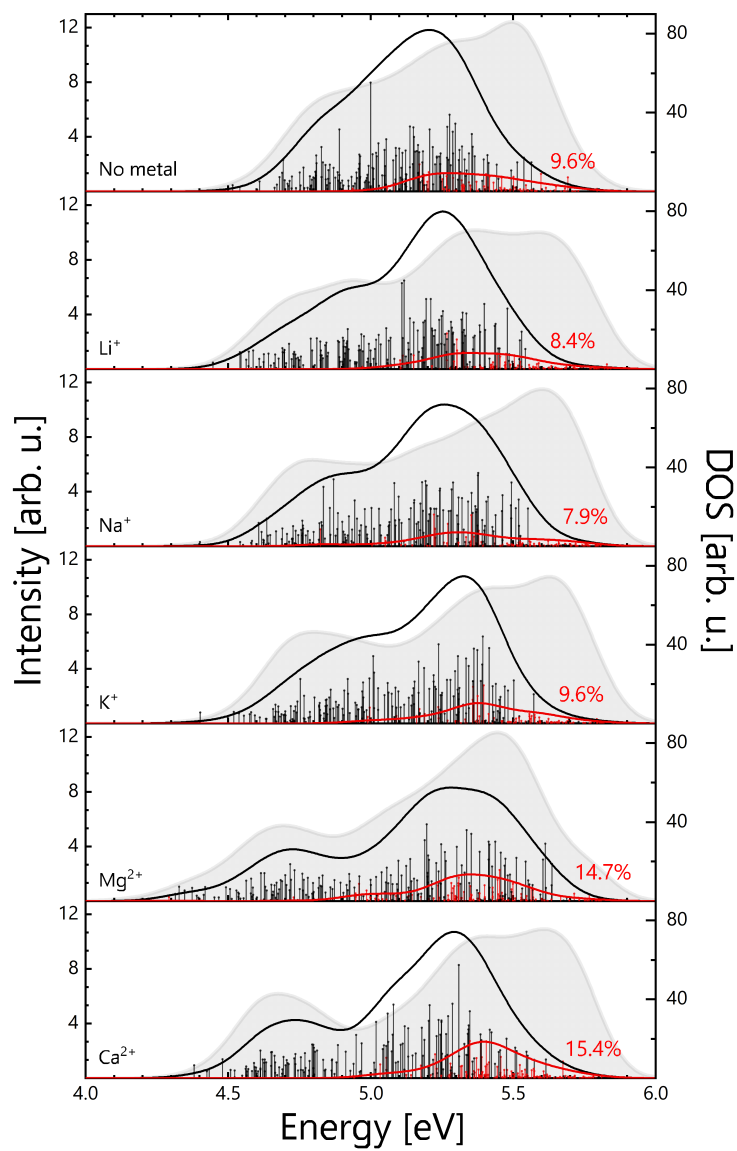
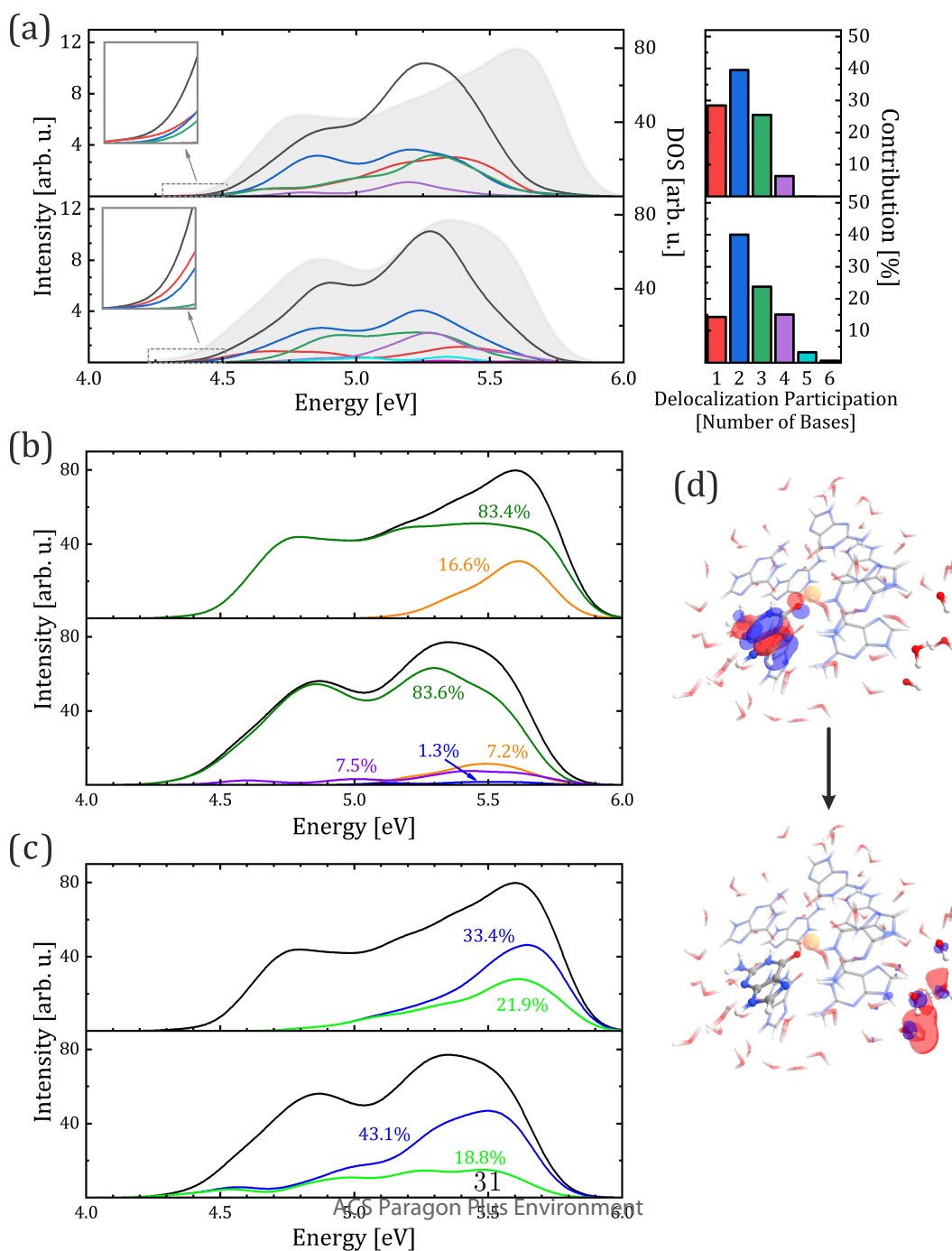
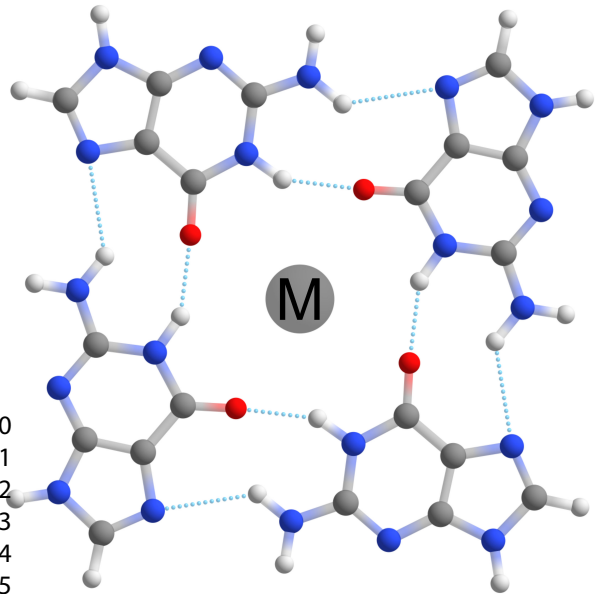


Figure (7) Excited state properties of of the G-octet templating with  $\text{Na}^+$  cation in the gas phase (upper plots) and aqueous solution (lower plots): a) Left: decomposition of absorption spectra (black lines) according to excited state delocalization:  $DEL = 1$  (red lines),  $DEL = 2$  (blue lines),  $DEL = 3$  (green lines),  $DEL = 4$  (purple lines),  $DEL = 5$  (cyan lines),  $DEL = 6$  (yellow lines). The insets show the decomposition of the absorption red tail. Density of states is represented by gray shaded area. Right: histograms of  $DEL$  contributions to the spectrum (the same coloring code as in the spectrum plots). b) Density of states (black line) decomposed on the  $\pi\pi^*$  (green line) and  $n\pi^*$  (orange line) states, charge transfer states between the G-octet and water (purple line) and transitions localized on water molecules (blue line). c) Density of states (black line), and its charge transfer (blue line) and charge separation (green line) states localized on the G-octet. d) Natural transition orbitals involved in a selected charge transfer from the G-octet to water molecules.



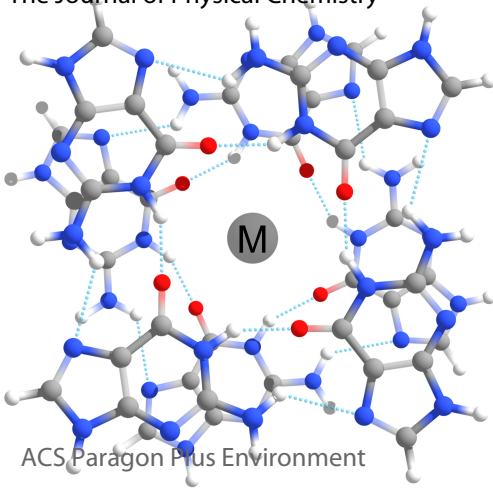


(a)

1  
2  
3  
4  
5  
6  
7  
8  
9  
10  
11  
12  
13  
14  
15

(b)

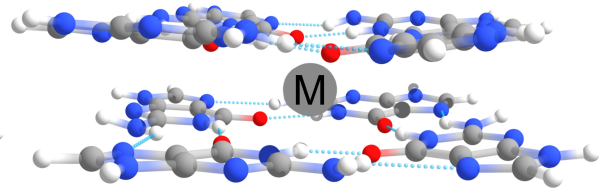
The Journal of Physical Chemistry



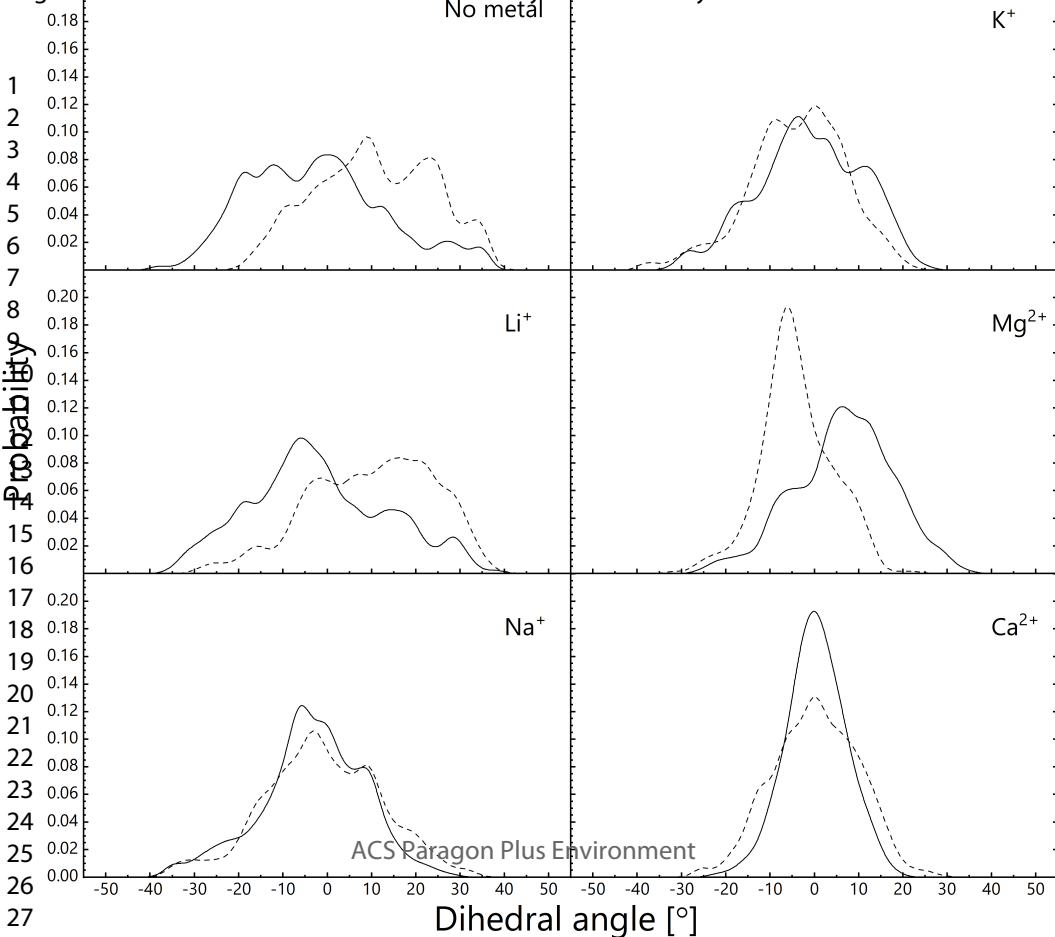
ACS Paragon Plus Environment

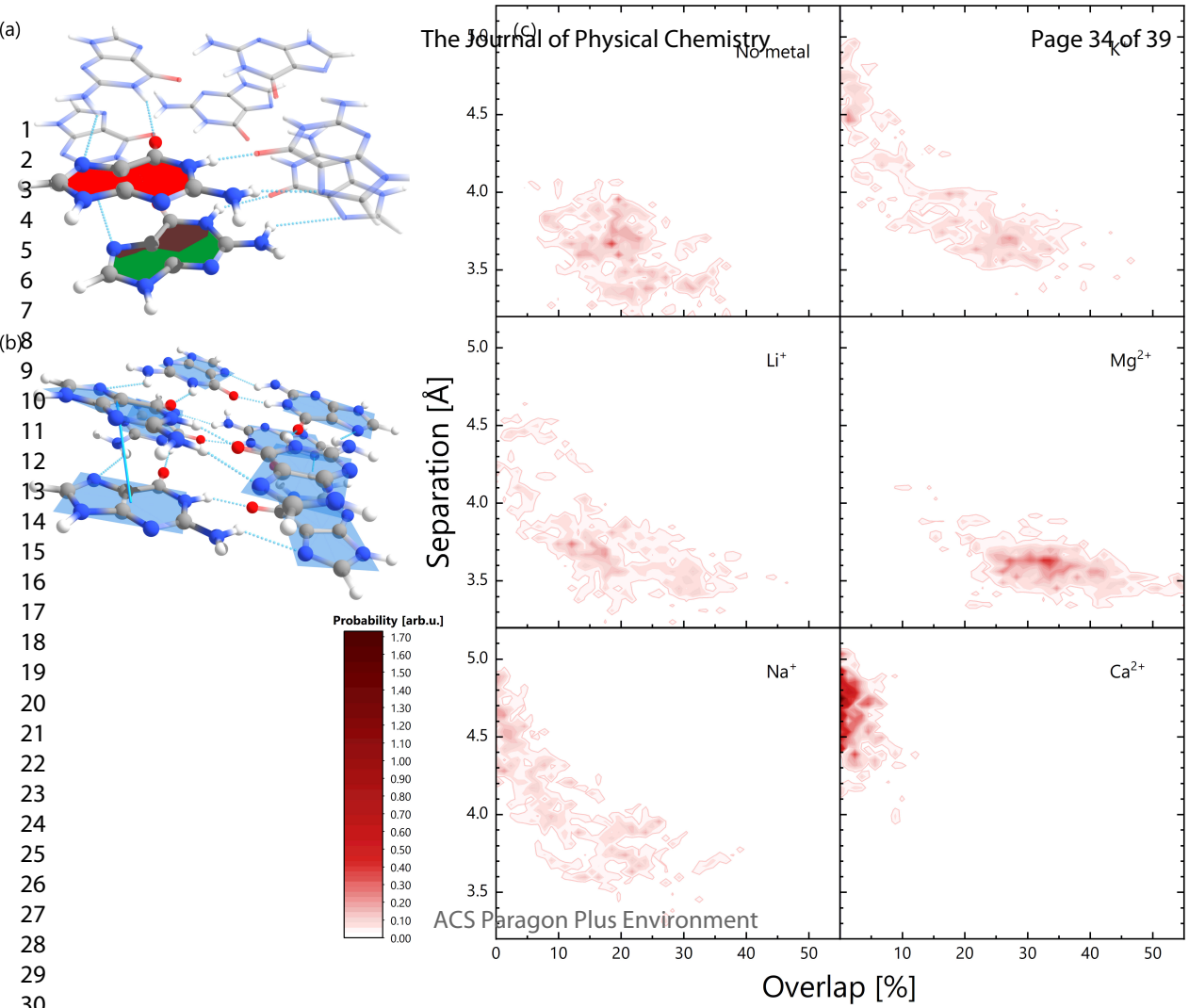
Page 32 of 39

(c)



No metal

 $K^+$ 1  
2  
3  
4  
5  
6  
7  
8  
15  
16  
17  
18  
19  
20  
21  
22  
23  
24  
25  
26  
27  
28



1  
2  
3  
4  
5  
6  
7  
8  
9  
19  
20  
21  
22  
23  
24  
25  
26  
27  
28  
29  
30  
31  
32  
33  
34  
35  
36

No metal

79.1%

20.9%

Li<sup>+</sup>

84.1%

15.9%

Na<sup>+</sup>

83.4%

16.6%

K<sup>+</sup>

81.6%

18.4%

Mg<sup>2+</sup>

90.6%

9.4%

Ca<sup>2+</sup>

97.5%

2.5%

ACS Paragon Plus Environment

4.0 4.5 5.0 5.5 6.0

Energy [eV]

